



# Mechanical properties of the weld line defect in micro injection molding for various nano filled polypropylene composites

Lei Xie\*, Gerhard Ziegmann

*Institute of Polymer Materials and Plastics Engineering, Technology University of Clausthal, Agricola str.6, 38678, Clausthal-Zellerfeld, Germany*

## ARTICLE INFO

### Article history:

Received 23 March 2010

Received in revised form 13 August 2010

Accepted 10 September 2010

Available online 22 September 2010

### Keywords:

Micro injection molding

Weld line

Carbon nanofibers

Titanium dioxide

Polypropylene

Tensile test

## ABSTRACT

The nano filled functional polymer materials have been widely processed with micro injection molding technology for micro electromechanical systems (MEMS) fabrication. As the unfavorable defect in micro injection molding parts, weld line brings reduced mechanical and physical properties, especially for nano filled composites. In this study, polypropylene (PP) was compounded respectively with carbon nano fibers (CNFs) and TiO<sub>2</sub> nano particles at various weight fractions (10, 20, 30, 35 wt%) through co-screws internal mixing. The morphological, thermal and rheological properties of nano composites were characterized by wider angle X-ray diffraction (WAXRD), different scanning calorimeter (DSC) and high pressure capillary rheometer. Additionally, under the constant setting of injection molding process parameters in injection molding machine, micro tensile samples with weld lines for each nano filled PP composite were produced. The tensile tests were served as the characterizing method for weld line mechanical properties. The results show that when the CNFs is filled higher than 10 wt%, the tensile strength of samples with weld lines made of nano composites become lower than neat PP. While the raising CNFs content contributes to the improved *E* modulus of micro injection molded weld lines. Additionally, with the increasing fraction of CNFs in PP, the weld line area's elongation percent is decreased. Whereas for case of TiO<sub>2</sub>, the 10 wt% is the threshold for micro injection molded weld line tensile strength turning from decrease trend to increase. The same as CNFs, elongation of micro weld line samples were in general lower than neat PP as well, due to the addition of TiO<sub>2</sub> nano particles.

© 2010 Elsevier B.V. All rights reserved.

## 1. Introduction

Many kinds of fillers are compounded with polymers in order to modify the thermal, physical and mechanical properties of the polymer matrix since tens of years ago. Particularly in case of nano filled composites (nano particles or fibers with the scale from 1 nm to as large as 100–200 nm), due to the same magnitude between polymer coils and nano fillers, molecular interaction between the polymer and the nano fillers will give polymer composites unusual properties that conventional polymers cannot possess [1–6]. With the emerge and development of micro injection molding process, this kind of amazing material is also applied in it for satisfying the special photonic, electrical, thermal and mechanical requirement of some smart functional micro system parts, e.g. micro gears, micro fuel cell bipolar plates, micro fluid analytic plates [7–10].

Nevertheless, as the evolutionary technology from conventional injection molding process, some defects that emerge in conventional case take place in micro injection molding as well. Weld line is one of them, which leads to reduced mechanical properties

and surface qualities. This defect is caused by multi injection gates, uneven mold cavity thickness and mold inserts [11], which is hardly be avoided whatever in conventional injection molding or in micro injection molding. Therefore, improving the strength of the weld line becomes one main task in injection molded parts production, which is related to many factors. As one of those relevant factors, the effect of fillers compounded in polymer matrix on weld line strength has been well investigated in conventional injection molding process [11]. Fisa and Rahmani [12] and Meddad and Fisa [13] studied the effect of cavity shape on the weld line strength in glass fiber reinforced polypropylene as a function of fiber concentration. But the results shown the weld line strength is independent of the cavity shape and is a function of fiber concentration only. Bouti and Fisa [14], Lalande [15] reported that the weld line strength in long-fiber-reinforced PP is extremely poor and decreases with fiber concentration. Nadkarni and Ayodhia [16] studied the effect of knit-lines on the mechanical behavior of unfilled and glass fiber-reinforced semicrystalline polymers, such as polypropylene, poly(butylene terephthalate), poly(ethylene terephthalate), and poly(phenylene sulfide). Unfilled and fiber-reinforced polystyrene was also investigated for reference. Based on the strength and strain to failure results, filler glass fibers significantly reduced the weld line in comparison to the respective unfilled grades polymers. How-

\* Corresponding author.

E-mail address: [Lei.Xie@tu-clausthal.de](mailto:Lei.Xie@tu-clausthal.de) (L. Xie).

**Table 1**

General properties of PP used in this study.

Properties	Values
Density (g/cm <sup>3</sup> )	0.9
MFR (g/10 min)	52 (230 °C/2.16 kg)
Tensile stress (MPa)	37
Heat deflection temperature (°C)	105 (0.65 MPa, unannealed)
VICAT softening temperature (°C)	152
Specific heat capacity (J/(g °C))	2.62 (126.85 °C)
Thermal conductivity (W/(m K))	0.2067 (125 °C)
Electrical conductivity (S/m)	2.81E–16 (25 °C)

ever, the investigation on the weld line mechanical properties in micro injection molding process is relative limited [17–20], and much less documented in the aspect of correlation between nano fillers and micro injection molded weld line strength.

Hence, according to the aforementioned literatures' research- ing achievements, the presented study is heading to investigate how nano fillers affect the mechanical properties of micro injection molded weld lines with various filler shape and loading fractions.

## 2. Experimental

### 2.1. Materials

#### 2.1.1. Polypropylene (PP)

PP (PPH 734–52 RNA) produced by DOW Europe GmbH was used as the polymer matrix of nano composites system and reference unfilled neat polymer in this study. The general properties of this PP are listed in Table 1.

#### 2.1.2. Carbon nano fibers (CNFs)

The CNFs were purchased from the company carbon NT&F 21® in Austria, which belong to the type of HT (heat treated) PR-24 carbon nano fiber (Pyrograf-IIIITM) produced by the vapor-grown carbon fiber production. The fiber length is ranging from 30 µm to 100 µm and its outer diameter is various from 80 to 150 nm. The SEM image of the CNFs bundles is shown in Fig. 1.

#### 2.1.3. TiO<sub>2</sub> nano particles

The TiO<sub>2</sub> nano particles are practical additives for polymers in order to satisfy with the applications consisting of high-voltage insulation, IC substrate boards, toners fluorescent tubes, toners, battery separators and UV sun screen lotion.

The TiO<sub>2</sub> nano particles used in this dissertation are Hombitec RM produced by the Sachtleben GmbH, which are spherical with about 20 nm diameter and 4 g/cm<sup>3</sup> density. Fig. 2 shows a TEM micrograph of TiO<sub>2</sub> nano particles at excessive agglomeration.

### 2.2. Nano PP composites compounding

One Thermo Haake® co-twin screws micro kneader was applied as the Nano composites compounding equipment, which can supply six temperature controlling zones in mixture chamber (48 cm<sup>3</sup>) up to 360 °C and a maximum torque 5 cN m. During the compounding process, with the various weight proportions, the polymer matrix PP and nano fillers were added into the kneader chamber in total amount of 40 g each time. First, PP was put into the heated chamber and held at 190 °C for roughly 2 min, then the nano fillers were fed into the chamber. After 25 min com-

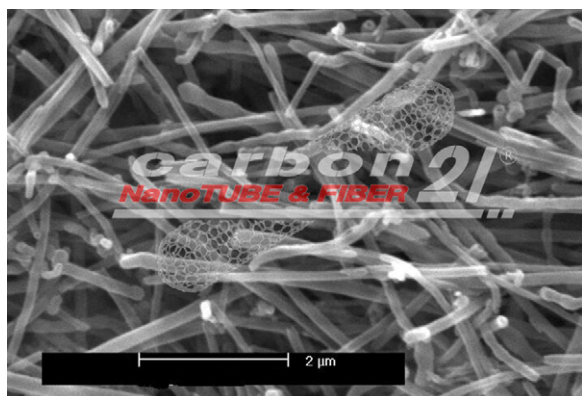


**Fig. 1.** SEM image of the carbon nanofibers used in the study.

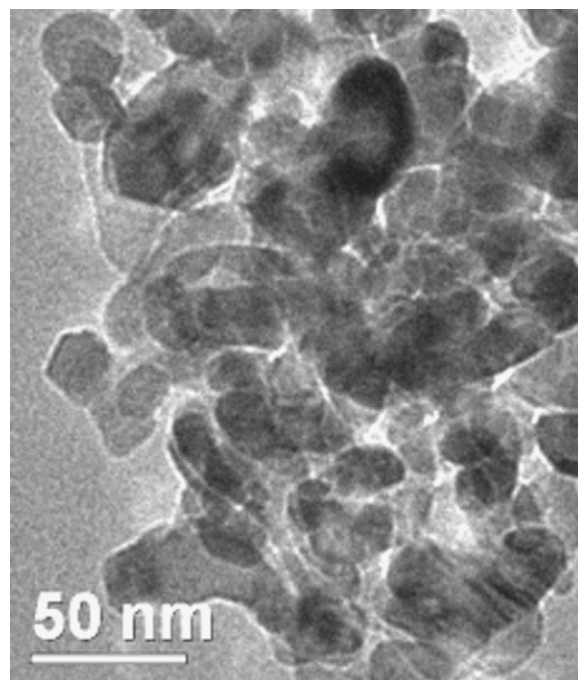


**Fig. 2.** TEM image of the TiO<sub>2</sub> nano particles used in the study.

pounding of the matrix and fillers at 60 rpm, the final composites were collected and granulated by a grinder for injection molding process in the next step. Granulates of nano composites to be used in micro injection molding process are displayed in Fig. 3. Based on this process, the nano PP composites with 10, 20, 30 and 35 wt% CNFs and TiO<sub>2</sub> nano particles were prepared respectively.

### 2.3. Characterization

Wide angle X-ray diffraction (WAXRD) measurements were performed on the Diffractometer Siemens D 5000 with Cu Kα radiation ( $\lambda = 0.1541$  nm) at room temperature atmosphere. During the test,  $2\theta$  was ranged from 5° to 65° at a scanning speed of 0.4°.

Differential scanning calorimeter (DSC) analysis was implemented on a TA instruments DSC1009 with a nitrogen atmosphere and a sample weight of  $10 \pm 2$  mg. Hermetically sealed sample containers were used in these experiments to avoid oxidation. The measurements were processed by a heat-cool-heat cycle. The sample was firstly heated up to 280 °C from room temperature at the heating speed of 10 °C/min, then was cooled down to 50 °C at the same temperature speed in order to record the crystallization process of the sample. Afterwards, it was heated up to 280 °C again at heating speed of 10 °C/min aiming to track the melting behavior of the sample.

The rheological property was characterized by a high pressure capillary rheometer from Goettfert GmbH (Rheograph 75) with max. force 75 kN. The nozzle used in the measurement has 15 mm length, 1 mm diameter of outlet hole and 90° feeding angle. The rheological testing was executed only on one single capillary without the second reference capillary, and the testing results were corrected by Rabinowitsch equations.

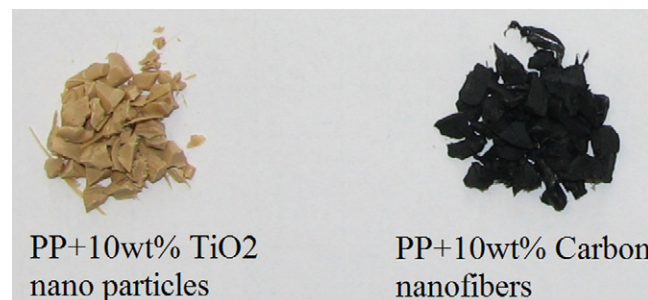


**Fig. 3.** Granulates of nano PP composites for micro injection molding process (at 10 wt%).

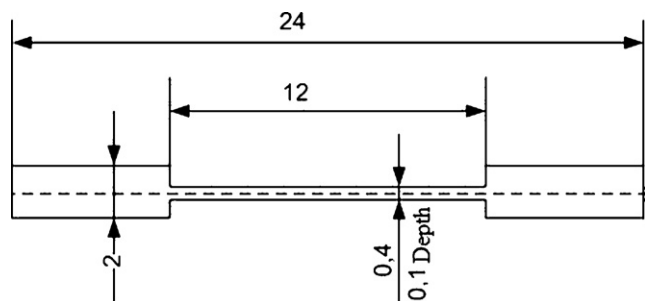


Fig. 4. The dimension and geometry of the micro tensile sample molded in this study (mm).

#### 2.4. Samples preparation

A horizontal injection molding machine (Arburg® 220S) was chosen as the experimental machine, which can supply 150 kN maximum clamping force and 250 MPa maximum injection pressure. Its screw diameter is 15 mm and minimum shot size is 0.5 cm<sup>3</sup>.

The micro dumb-bell tensile specimen was chosen as the objective part, whose geometry and dimension are demonstrated in Fig. 4. One double-gated mold with this part cavity was designed and constructed, which is shown in Fig. 5. In order to avoid the short-shot of the micro cavity during injection molding process, a variotherm mold temperature control unit was integrated in [21].

All the compounded nano composites were processed by Arburg® 220S injection molding machine to form the micro tensile samples with intended weld lines in middle of the sample. During the experiments, the processing parameters were fixed setting in the injection molding machine as the following: the melt temperature 230 °C, the mold temperature 150 °C, the injection pressure 100 MPa, the injection speed 20 cm<sup>3</sup>/s and the ejection temperature 60 °C. In order to guarantee the process repeatability [22–24], every process batch was implemented 50 times, the molded samples from first and last 10 times were abandoned and only the samples get in middle 20 times were collected for tensile testing in the next step.

#### 2.5. Tensile test

Weld line strength of micro tensile samples were tested on the multi-function mechanical test machine (Zwick®). The test cell load is 20 N, the distance between two sample holding crossheads 13.8 mm, and tensile speed 1 mm/min. The tensile strength was recorded by the Testxpert® software automatically. The measurement was repeated at least 5 times for samples from the same production batch and the average of five sample readings was taken for accurate results.

### 3. Results and discussion

#### 3.1. WXRD analysis

The WXRD measuring patterns of unfilled PP and nano filled PP composites are shown in Fig. 6. The feature X-ray diffracting peaks of pure PP were displayed at  $2\theta = 13.88^\circ$ ,  $16.64^\circ$ ,  $18.61^\circ$ ,  $21.02^\circ$ ,  $21.56^\circ$ ,  $25.2^\circ$  and  $28.48^\circ$ , which are respectively corresponding to

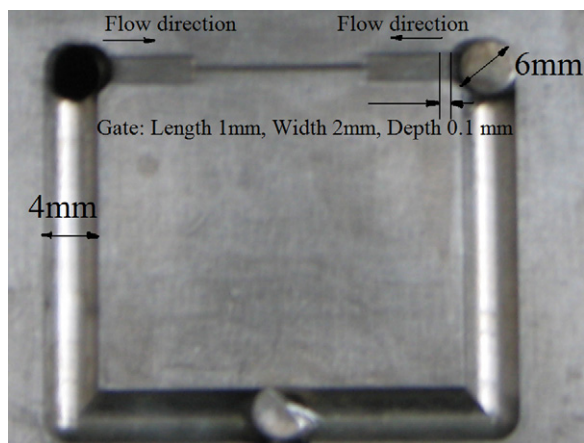


Fig. 5. The cavity location and runner system arrangement in the real case.

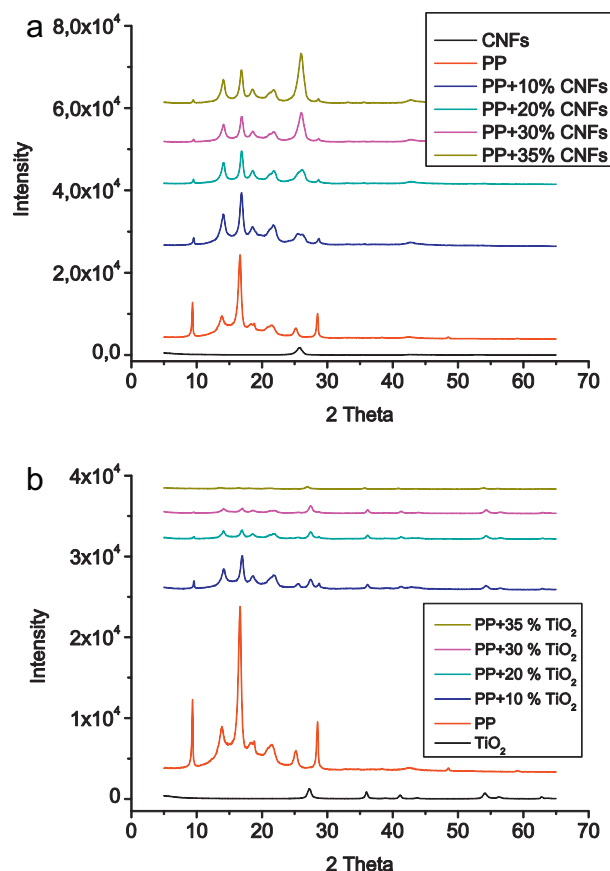


Fig. 6. WXRD patterns of PP and CNFs filled PP (a); TiO<sub>2</sub> filled PP (b).

the (1 1 0), (0 4 0), (1 3 0), (1 1 1), (0 4 1), (0 6 0) and (2 2 0) diffraction planes of PP  $\alpha$ -form crystal morphology. The feature diffraction peaks of Carbon nanofibers and TiO<sub>2</sub> nanoparticles are observed at  $2\theta = 25.76^\circ$  (CNFs) and  $27.24^\circ$  (TiO<sub>2</sub>).

According to the XRD traces, the crystal form of PP was not changed after adding nano fillers, since there are no feature peaks appeared corresponding to  $\beta$  and  $\gamma$  form crystals of PP. However, with the addition of nano fillers, the position of the PP  $\alpha$ -form peaks was shifted rightward to larger  $2\theta$  angle slightly, and the intensity of those peaks changed more or less.

By Bragg equation [25], the distance between diffraction planes of crystals can be calculated:

$$d_{hkl} = \frac{n\lambda}{2 \sin \theta} \quad (1)$$

where  $n$  is the diffraction level related to the crystal form;  $\lambda$  is wavelength of the irradiation X-ray source;  $\theta$  is the Bragg angle.

The crystallite size perpendicular to the diffraction plane (lattice planes) can be obtained by the Scherrer equation [25]:

$$L_{hkl} = \frac{k\lambda}{\beta_{hkl} \cos \theta_{hkl}} \quad (2)$$

where  $k$  is shape factor associated with the crystallites (assumed as 0.9 here);  $\lambda$  is wavelength of the irradiation X-ray source;  $\theta$  is the Bragg angle and  $\beta_{hkl}$  is the half height of the feature peak (rad).

According to Eqs. (1) and (2), the fact based on XRD patterns that can be found is that, with loading of CNFs and nano TiO<sub>2</sub> particles, the distance among the diffraction lattice planes of PP crystallites is slightly decreased in general. By adding 10 wt% CNFs, due to the increment of feature peak half height, the crystallite size of  $L_{hkl}$  perpendicular to the (1 1 0), (1 3 0), (1 1 1) and (0 4 1) plane are smaller than those of pure PP. As the loading content of CNFs increases up



**Table 2**

Peak temperature of crystallization melting ( $T_m$ ) and peak temperature of crystallization ( $T_p$ ) of PP and nanofilled PP composites.

Materials	$T_m$ (°C)	$T_p$ (°C)
PP	169.20	124.28
PP + 10 wt% CNFs	164.93	127.69
PP + 20 wt% CNFs	164.65	129.96
PP + 30 wt% CNFs	164.65	132.52
PP + 35 wt% CNFs	164.08	132.52
PP + 10 wt% TiO <sub>2</sub>	166.64	127.40
PP + 20 wt% TiO <sub>2</sub>	165.60	129.68
PP + 30 wt% TiO <sub>2</sub>	165.60	129.39
PP + 35 wt% TiO <sub>2</sub>	166.90	129.11

to 20% and 30%, the crystallite size of those planes becomes larger than the case of unfilled PP, but it is getting smaller again when the loading fraction reaches 35 wt%. The reason for this fact can be that as adding 10 wt% CNFs in PP, the CNFs restrict the PP molecular to form large size crystals, however when filling more CNFs in PP at 20 wt% and 30 wt%, the nucleation effect of CNFs is getting obvious, the resulting larger size crystals of PP are formed. Nevertheless, continuously adding CNFs up at 35%, the increased fibers' aggregation as well as the dramatically decreased distance among fibers reduced the nucleation effect of nano fibers and give more restriction for large size crystals forming. The intensity of diffraction feature peaks corresponding to the (040) and (220) crystal plane of  $\alpha$  form is decreased; the resulting crystallite size is larger than that of neat PP.

One more fact worthy to mention is that from 10 wt% to 30 wt% of CNFs, the intensity of all diffraction peaks for PP/CNFs composites is reduced with increment of the loading content, but it increases again at 35 wt%, because at high fitting content, the increasing agglomeration of nano fibers decreases their effect on PP matrix, which makes the instinct feature peaks of PP get obvious again.

Regarding to TiO<sub>2</sub> nano particles, with their addition in PP matrix, the intensity of all diffraction feature peaks for PP/TiO<sub>2</sub> composites are reduced gradually as the loading fraction increases, but the half heights of the feature peaks become larger, which means the crystallite size of  $\alpha$  form in PP becomes larger.

Additionally, for all nano filled PP composites, new diffraction peaks near  $2\theta = 25.76^\circ$  and  $27.24^\circ$ , corresponding to CNFs and TiO<sub>2</sub> respectively. For CNFs, the intensity of the feature peak is increased as the CNFs loading content increases. And the feature peak of  $\alpha$  form in the plane (060) was replaced by the feature peak of CNFs after 10 wt% due to the raising amount of CNFs. Furthermore, comparing with the pure CNFs, the feature peak of CNFs in PP/CNFs composite shows higher intensity, which is proportional to loading contents. For TiO<sub>2</sub>, only 10 wt% of TiO<sub>2</sub> addition enhanced the intensity of its feature peak than that of pure TiO<sub>2</sub> nano particles. From 20 wt%, the intensity of this feature peak starts to decrease and lower than the case of pure TiO<sub>2</sub>, which means the larger crystallite size appear associated with the agglomeration of the nano particles in polymer matrix.

### 3.2. DSC analysis

With DSC measurements, the peak temperature of crystallization melting ( $T_m$ ) and the peak temperature of crystallization ( $T_p$ ) were obtained and listed in Table 2. It implies that the addition of nano fillers lead to higher peak temperature of crystallization melting ( $T_m$ ), but increasing the loading fraction above 10 wt% does not result in a further increment of  $T_m$ . The reason for this is that the polymer chains in nano filled PP composites are relative smaller than in pure PP because the nano fillers restrict the formation of a large polymer chain and make them smaller ones, which contributes to make the melting temperature of materials lower.

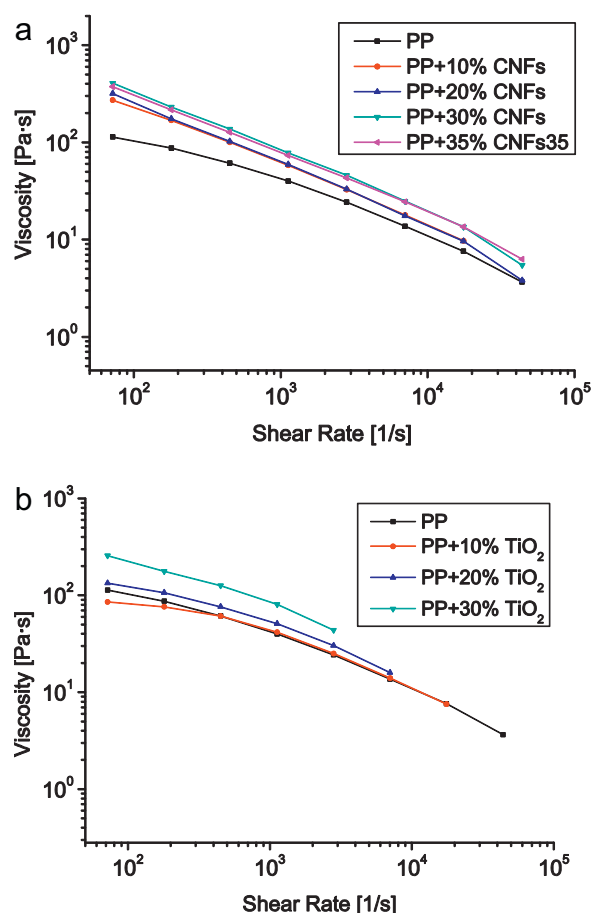


Fig. 7. Viscosity-shear rate curves for PP and nano filled PP composites.

The peak temperature of crystallization of PP was increased due to adding nano fillers, which is the result from the action of nano fillers as nucleating agents for PP crystals. However, there is a limiting effect of nucleating crystallization happened when the loading content is higher than 30 wt% for CNFs and 20 wt% for nano TiO<sub>2</sub>. Based on the comparison of  $T_m$  between PP/CNFs composites and PP/TiO<sub>2</sub> composites, CNFs show stronger nucleating performance for promoting heterogeneous nucleation than TiO<sub>2</sub> nano particles. This result indicates that CNFs has better dispersion in PP matrix than TiO<sub>2</sub> nano particles, which is also supported by the XRD pattern analysis for the crystallite size of CNFs and TiO<sub>2</sub> in PP from the section above.

### 3.3. Rheological property

The viscosity-shear rate curves after Rabinowitsch correction obtained by high pressure capillary rheometer are displayed in Fig. 7. From the results in Fig. 7, it is clear that the viscosity of nano filled PP is generally higher than neat PP. Higher nano fillers loading fraction causes higher viscosity. At the same concentration, CNFs filled PP shows higher viscosity than TiO<sub>2</sub> filled PP, which is because CNFs bring more flowing restriction than TiO<sub>2</sub> nano particles attributed by the more intensive interaction of carbon nanofibers and nanofibers-polymer chains.

### 3.4. Mechanical properties of micro injection molded weld lines

The compounded nano PP composites were processed by micro injection molding process for preparing the micro tensile samples

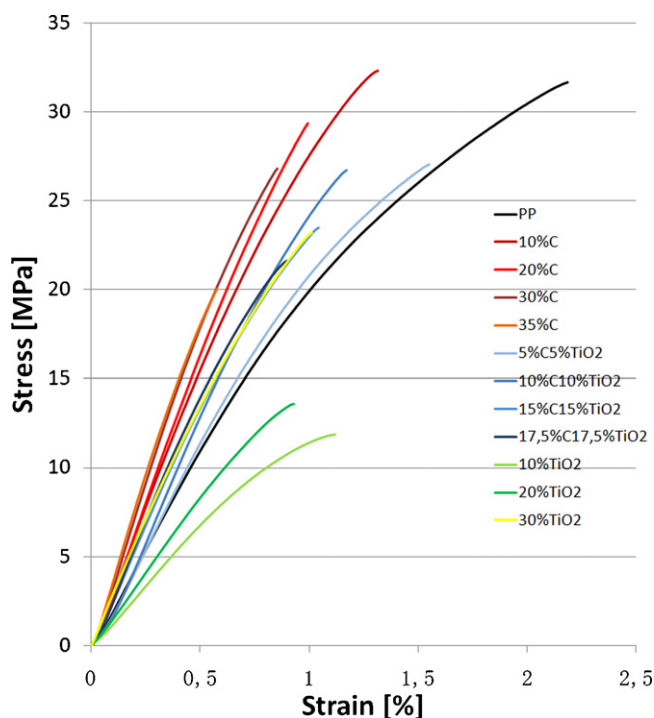


**Fig. 8.** Tensile test strain–stress curve of micro weld lines samples with various nano filler concentrations.

with intended weld lines. Then mechanical properties of formed samples were assessed by tensile testing with the characterizations of tensile strength,  $E$  modulus and elongation percent. It should be mentioned that due to the extremely brittleness of samples made of 35 wt%  $\text{TiO}_2$ /PP composites, there was no decent integrated samples able to be ejected during the micro injection molding process. Thus, the tensile test for this kind of composites was not implemented.

Testing results are plotted in Figs. 8–11. Fig. 8 shows the tensile strain–stress curves of neat PP and PP nano composites with various loading fractions. Due to the occurring of weld lines, there are no plasticity regions but elastic response regions for all tensile curves, which are similar to the results reported in the normal injection molding process [11]. The filling of nano fillers apparently aggravated the brittleness of micro tensile samples related to weld lines.

Fig. 9a demonstrates that with the weld line presenting, micro tensile samples of CNFs filled PP composites performed higher  $E$  modulus than the case of neat PP. The significant increase of  $E$  modulus of micro injection molded weld line can be observed when the CNFs were added into PP. And with the concentration of the nanofibers increasing, the responded  $E$  modulus of micro weld lines is increased. The increment of  $E$  modulus was not really marked from the comparison between 10 wt% and 20 wt% CNFs concentrations. However, when the loading fraction of CNF is higher than 20 wt%, the impressive enhancement of  $E$  modulus was exhibited. At 30 and 35 wt% of CNFs, comparing with neat PP, the 70% and 86% increase in  $E$  modulus of is presented respectively.

Whereas, compared with those of CNFs/PP composites, the  $\text{TiO}_2$  nano particles show different effects on micro weld line samples'  $E$  modulus. Weld line samples'  $E$  modulus are not increased but decreased due to the nano particles filling. However, with the increment of  $\text{TiO}_2$  nano particle's concentration, the  $E$  modulus is getting higher after the fraction at 10 wt% and at 30 wt%, it reaches the level higher than unfilled PP.

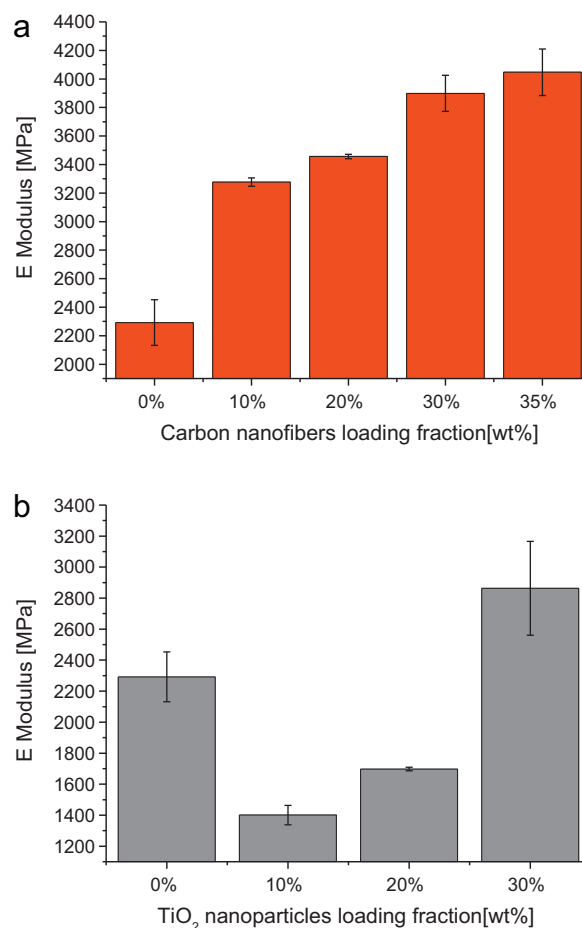


**Fig. 9.** (a)  $E$  modulus of micro weld lines samples with various CNFs concentrations; (b)  $E$  modulus of micro weld lines samples with various  $\text{TiO}_2$  nano particles concentrations.

Tensile strength was named as the assessing characterization of the micro injection molded weld line strength, and the testing results are displayed in Fig. 10, where it can be observed that with filling the CNF, the tensile strength of the sample was reduced in general than the case of pure PP, except for 10 wt% CNF/PP composites. Higher nanofibers contents lead to lower micro weld lines tensile strength. At 35 wt% CNF, the weld line strength was decreased dramatically compared to the other filling fractions. Regarding to  $\text{TiO}_2$ /PP nano composites, like the correlation between  $E$  modulus and loading contents of  $\text{TiO}_2$  particles, the 10 wt% is also the critical content for tensile strength turning from decreasing trend to increasing. When the particle content rises to 30 wt%, the tensile strength is close to the value at 30 wt% of CNFs.

Fig. 11 shows the correlation between nano fillers loading fraction and the weld line tensile sample's elongation percent. Normally the tensile elongation percent of PP is relative high. With appearance of weld lines, the deformation percent will be radically decreased. In this study, the micro tensile sample with weld line made of unfilled PP showed 2.17%. With increasing CNFs content, the value of elongation for weld line samples was reduced more intensively, to 0.57% at the 35 wt% of CNF content; as for  $\text{TiO}_2$  nano particles, by 10 wt% filling of  $\text{TiO}_2$ , the elongation percent is decreased obviously, however as the filling fraction of  $\text{TiO}_2$  increasing, the degree of decrement was not evident changed, the elongation percent was 1.11% at 10 wt% loading of  $\text{TiO}_2$  and 1.01% at 30 wt% loading of  $\text{TiO}_2$ .

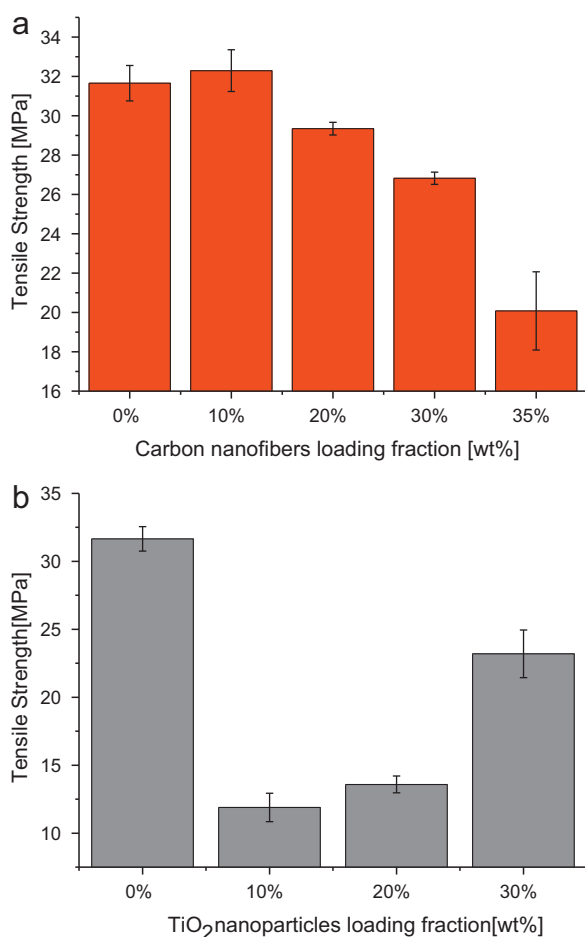


**Fig. 10.** (a) Tensile strength of micro weld lines samples with various CNFs concentrations; (b) tensile strength of micro weld lines samples with various TiO<sub>2</sub> nano particles concentrations.

## 4. Discussion

### 4.1. Effect of CNFS

As well known, except for low or ultra low wt% (<1 wt%), the tensile ductility of polymer matrix is deteriorate considerably by adding CNFs, which can be the results from modifications in the crystalline fraction of the polymer matrix or increasing agglomeration of CNFs within polymer matrix [26–28]. The fact of improved *E* modulus and reduced elongation of micro weld line tensile samples suggests that there are the same effects of CNFs on micro weld lines ductility as the case without it. Additionally, the more isotropic complex distribution and orientation of nano fibers in weld line areas contribute to more restriction sites preventing the polymer from deformation, therefore resulting in a decrease in ductility and an increase in brittleness of micro injection molded weld lines with PP/CNFs.

The decreased tensile strength of micro weld lines by loading CNFs could be caused by the nano fillers aligning perpendicular to the flow direction at the weld line and their non-uniform distribution, which is similar as the results reported in conventional injection molded weld line study [11]. Additionally, the planar orientation of nano fillers may also hinder molecular chain motion on solidification and inhibit optimal crystalline development and orientation in the weld line region.

As the nano fibers content increasing, the fiber's perpendicular orientation to the overall melt flow direction at weld line plane

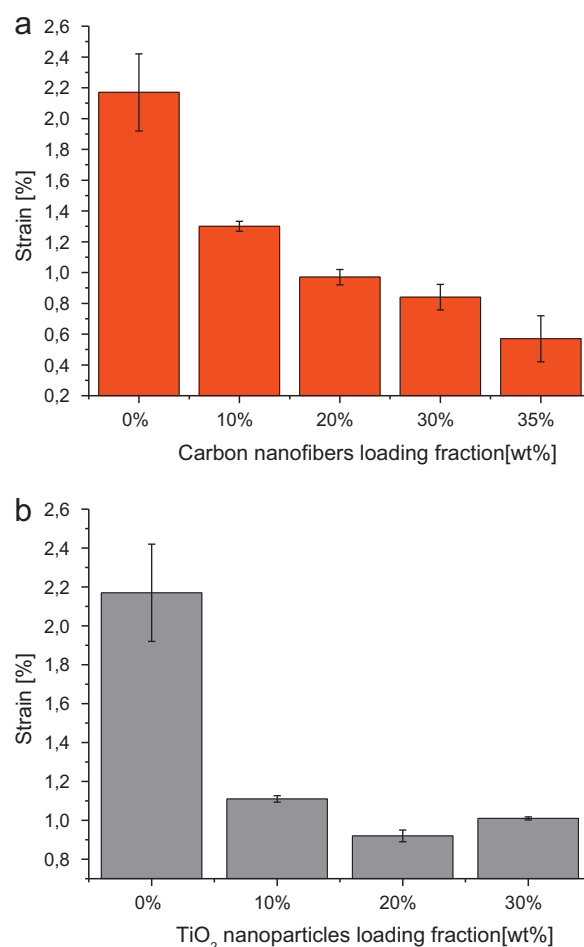


**Fig. 11.** (a) Elongation percent of micro weld lines samples with various CNFs concentrations; (b) elongation percent of micro weld lines samples with various TiO<sub>2</sub> nano particles concentrations.

will be more, hence more polymer chains are induced to orient in the same way. When both the flow fronts impinge at the weld line, the nanofibers and polymer chains together orient perpendicular to the flow direction, which will make a weld line with lower strength, hence the 35 wt% case showed the worst weld line strength. In Fig. 12, it is obviously illustrated that when carbon nanofibers weight content is higher than 20%, there are many orientations of nano carbon fibers perpendicular to the flow direction in weld line areas, and their footprints were evident.

As for 10 wt% CNF/PP composites system it shows a relative higher tensile strength than neat PP, because when the fiber filling grade is relatively low, at the weld line a small amount of nano fibers may align parallel to flow direction and across the weld line due to the higher shear rate in micro injection molding process, which will work as an enhancement for weld lines' tensile strength. Fig. 12b shows at 10 wt% of nano fibers, pull out holes and broken marks of nano fibers crossing weld lines are distributed widely in the weld line broken sections.

### 4.2. Effect of TiO<sub>2</sub> nano particles

For the phenomena of unexpected decreased *E* modulus at 10 and 20 wt% of TiO<sub>2</sub> filling in PP, the reason could be that at relative lower concentration the aggregation of TiO<sub>2</sub> nano particles reduced the theoretical performance of nano particle in enhancing polymer matrix stiffness which is predicted by Halpin-Tsai theory under perfect dispersion assumption [29]. However, with the filler



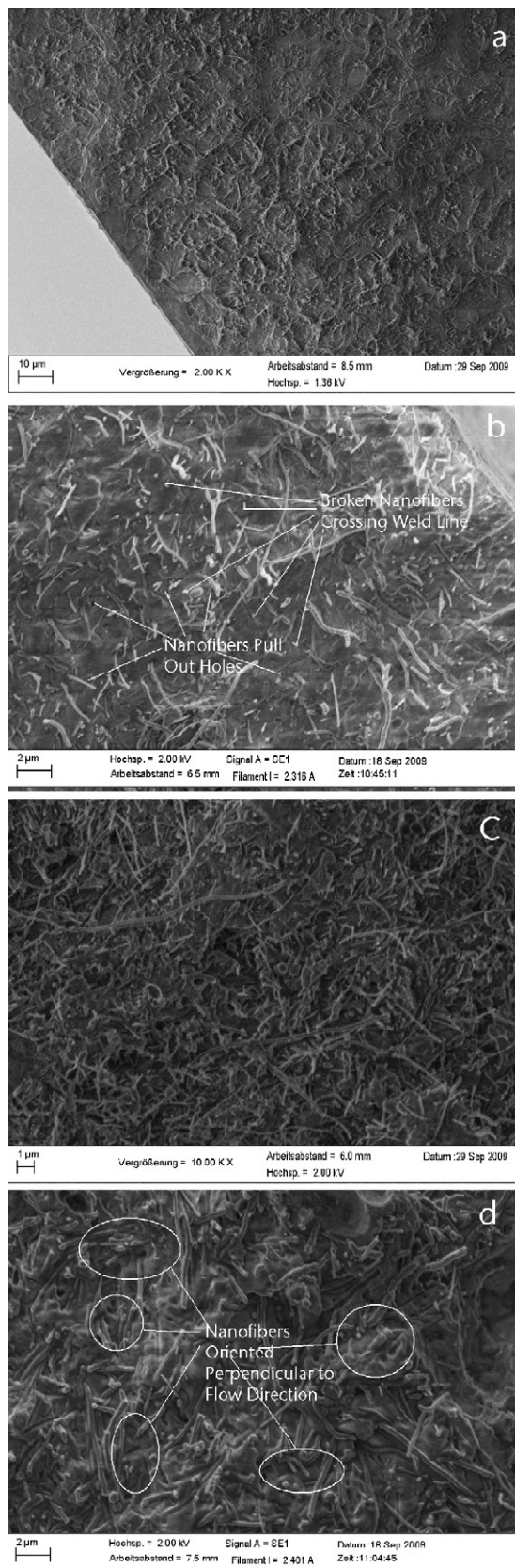


**Fig. 12.** SEM images of weld line samples tensile test broken section for various wt% CNFs filled composites: (a) neat PP; (b) PP + 10% carbon nano fibers; (c) PP + 20% carbon nano fibers; (d) PP + 30% carbon nano fibers; (e) PP + 35% carbon nano fibers.

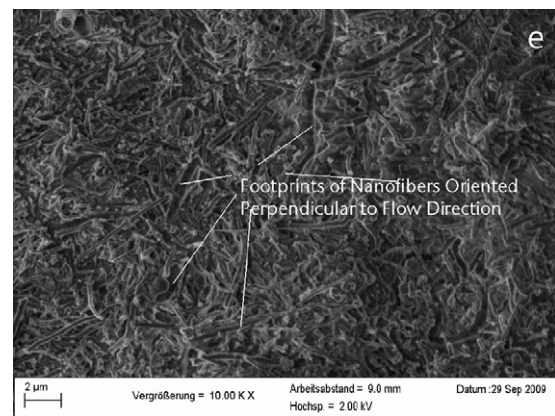


**Fig. 12.** (Continued)

contents increasing, the aggregation of particles is relatively limited increased, thus there are more chances for nano particles to be well dispersed in matrix and induce the occurrence of polymer chains intercalations which will improve the stiffness even there are still agglomeration existing. The SEM images in Fig. 13 clearly shows the distribution situation of particles at 10 wt% and 30 wt% of TiO<sub>2</sub> nano particles, which can support the explanation above.

Same as CNFs/PP composites, the tensile strength of TiO<sub>2</sub>/PP composites is lower than that of unfilled PP, which is also because the more direct interconnections among nano particles in weld line areas. Due to the similar influencing mechanism of nano particles on *E* modulus, at 30 wt% loading of TiO<sub>2</sub> nano particles, the

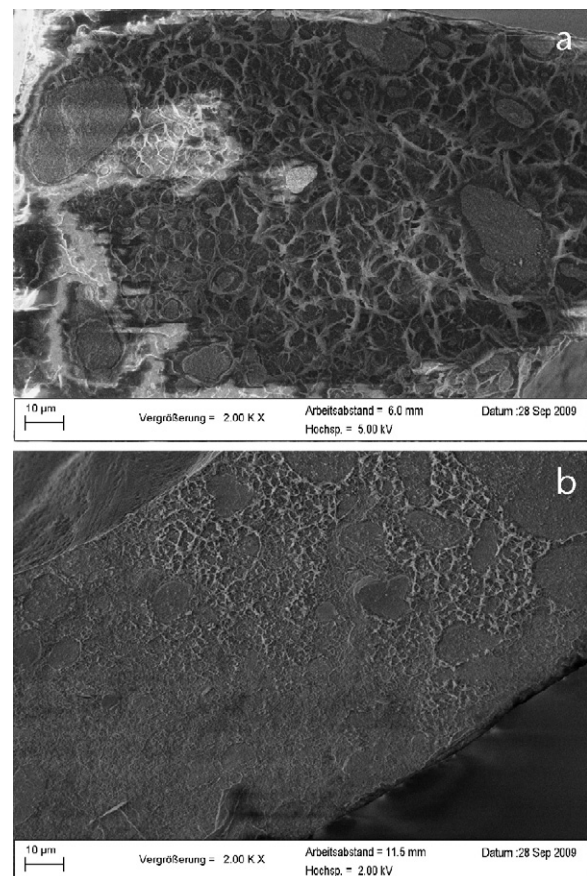


**Fig. 13.** SEM morphology of PP/TiO<sub>2</sub> nano composites with different loading contents: (a) 10 wt%; (b) 30 wt%.

increment of TiO<sub>2</sub> loading causes no further decreasing of tensile strength for micro weld line samples, but increases it.

In general, the ductility of micro weld line samples was decreased by adding nano particle of TiO<sub>2</sub>, but the stiffness was increased at high loading fraction (30 wt%).

#### 4.3. Weld line strength modeling

We assume that the micro injection molded weld line strength with nano filled PP is a function of nano filler's concentration only. Based on the tensile test results in this study, a second order polynomial weld line predicting equation was obtained by Newtonian iteration fitting method, shown as Eq. (3).

$$\delta_w = a\varphi^2 + b\varphi + \delta_m \quad (3)$$

where  $\delta_w$  is weld line strength,  $\varphi$  is the nano filler concentration,  $a$  and  $b$  are constant coefficients related to the filler features (filler's aspect ratio, dispersion situation etc.),  $\delta_m$  is tensile strength of polymer matrix. This empirical equation is supposed to predict the micro weld line strength in case of higher nano filler contents than 10 wt%, since in lower content (<1 wt%) the influence of nano fillers is conversely different according to reported literatures [26].

## 5. Conclusions

PP/CNFs and PP/TiO<sub>2</sub> composites with relative high loading fractions (10, 20, 30 and 35 wt%) were fabricated by inner melt mixing process. Micro tensile test samples were formed by injection molding combined with variotherm process for all composites, except for 35 wt% TiO<sub>2</sub> filled PP. The morphological properties of all nano composites were characterized by WXR, whose results imply the adding nano fillers did not change the crystal form of PP, but the crystallites size and distance between lattices of crystals were changed with various nano fillers and loading fractions. DSC analysis show that due to the nucleating function of nano fillers, the peak temperature of crystallization was increased and the peak temperature of crystallization melting was decreased by adding the nanofillers. The flow ability of nano composites was tested by high pressure single capillary rheometer and the results demonstrate that nano fillers increased the viscosity of PP matrix. Based on these significant information and analysis foundation of the nano filled composites, the micro weld line samples were formed by injection molding process and characterized by tensile test method. From the achieved results, it can be found that in general, for functional nano filled polymer composites, the mechanical property of micro weld lines were obviously influenced by nano fillers' shape and loading fractions. The  $E$  modulus of micro weld line was increased due to loading CNFs in PP matrix, while the elongation of the micro tensile samples with weld line is considerably decreased comparing with those of unfilled PP samples. The detrimental tensile strength

of micro weld lines were observed when CNFs contents increasing, except for at a 10 wt%. For TiO<sub>2</sub> nano particles filled PP, due to the poor dispersion of nano particles, at low loading fraction of 10 wt%, the  $E$  modulus and tensile strength of micro weld lines were decreased by filling nano particles, but when the loading fraction is increased to 30%, the  $E$  modulus and tensile strength of micro weld line were increased again compared with the low loading level. Finally, an empirical prediction equation for micro injection molded weld line strength of nano PP composites was proposed for higher nano filler loading fraction than 10 wt%.

Further investigation on this topic might be done in lower nano filler wt% contents (<1 wt%) range.

## Acknowledgement

The authors would like to thank DFG (Deutsche Forschungsgemeinschaft) for giving the financial support to the investigation.

## References

- [1] J.H. Woo, Polymer Nanocomposites: Processing, Characterization and Applications, McGraw-Hill, New York, 2006.
- [2] K. Lozano, S.Y. Yang, Q. Zeng, J. Appl. Polym. Sci. 93 (2004) 1500.
- [3] C.K. Huang, Eur. Polym. J. 42 (9) (2006) 2174.
- [4] M. Knite, I. Klemenok, G. Shakale, V. Teteris, J. Zicans, J. Alloys Compd. 434–435 (2007) 850–853.
- [5] P. Zhang, H.P. Zhang, Z.H. Li, Y.P. Wu, T. van Ree, Polym. Adv. Technol. 20 (6) (2009) 571.
- [6] W.S. Jou, H.Z. Cheng, C.F. Hsu, J. Alloys Compd. 434–435 (2007) 641–645.
- [7] L. Merz, S. Rath, V. Piottter, R. Ruprecht, J. Ritzhaupt-Kleiss, J. Hausselt, Microsyst. Technol. 8 (2–3) (2002) 129.
- [8] T. Gietzelt, V. Piottter, O. Jacobi, R. Ruprecht, J. Hausselt, Adv. Eng. Mater. 5 (3) (2003) 139.
- [9] B. Su, T.W. Button, A. Schneider, L. Singleton, P. Prewett, Microsyst. Technol. 8 (4–5) (2002) 359.
- [10] C.K. Huang, S.W. Chiu, J. Appl. Polym. Sci. 98 (5) (2005) 1865.
- [11] S. Fellahi, A. Meddad, B. Fisa, B.D. Favis, Adv. Polym. Technol. 14 (3) (1995) 165.
- [12] B. Fisa, M. Rahmani, Polym. Eng. Sci. 31 (18) (1991) 1330.
- [13] A. Meddad, B. Fisa, Polym. Eng. Sci. 35 (11) (1995) 893.
- [14] A. Bouti, B. Fisa, SPE ANTEC Tech. Papers 37, 1991, p. 2112.
- [15] F. Lalande, SPE ANTEC Tech. Papers 37, 1991, p. 404.
- [16] V.M. Nadkarni, S.R. Ayodhia, Polym. Eng. Sci. 33 (6) (1993) 358.
- [17] L. Xie, G. Ziegmann, Microsyst. Technol. 15 (6) (2009) 913.
- [18] L. Xie, G. Ziegmann, Microsyst. Technol. 15 (7) (2009) 1031.
- [19] G. Tosello, A. Gava, H.N. Hansen, G. Lucchetta, F. Marinello, Wear 266 (5–6) (2009) 534.
- [20] L. Xie, G. Ziegmann, Microsyst. Technol. 15 (6) (2009) 1427.
- [21] L. Xie, G. Ziegmann, Microsyst. Technol. 14 (6) (2008) 809.
- [22] A. Jungmeier, K. Vetter, G.W. Ehrenstein, 4M 2009 Conference, doi:10.1243/17547164C0012009011.
- [23] G. Tosello, G. Lucchetta, H.N. Hansen, A. Gava, S. Paliuri, 4M 2009 Conference, doi:10.1243/17547164C0012009045.
- [24] A. Jungmeier, I. Kuehnert, G.W. Ehrenstein, T.A. Osswald, ANTEC (2009) 1328–1332.
- [25] H.P. Klug, L.E. Alexander, X-ray Diffraction Procedures for Polycrystalline and Amorphous Materials, 2<sup>nd</sup> ed., Wiley, New York, 1974.
- [26] S.P. Bao, S.C. Tjong, Polym. Compos. 30 (2009) 1749.
- [27] H.X. Jiang, Q.Q. Ni, T. Natsuki, Polym. Compos. (2009), doi:10.1002/pc.20897.
- [28] K. Lozano, E.V. Barrera, J. Appl. Polym. Sci. 79 (2001) 125.
- [29] J.C. Halpin, J.L. Kardos, Polym. Eng. Sci. 16 (1976) 334.